DALTON
FULL PAPER

Relative basicities of the oxygen atoms of the Linquist polyoxometalate $[Mo_6O_{19}]^{2-}$ and their recognition by hydroxyl groups in radical cation salts based on functionalized tetrathiafulvalene π donors

Anne Dolbecq,[a] Aude Guirauden,[a] Marc Fourmigué,[a] Kamal Boubekeur,[a] Patrick Batail,*[a] Marie-Madeleine Rohmer,[b] Marc Bénard,[b] Claude Coulon,[c] Marc Sallé[d] and Philippe Blanchard[d]

[a] *Institut des Matériaux de Nantes, UMR 6502 CNRS-Université de Nantes, BP 32229, 2, rue de la Houssinière F-44322 Nantes Cedex 03, France. E-mail: batail@cnrs-imn.fr*
[b] *Laboratoire de Chimie Quantique, UMR 7551 CNRS-Université Louis Pasteur, F-67000 Strasbourg, France*
[c] *Centre de Recherches P. Pascal (CRPP), CNRS, av. Dr. Schweitzer, F-33600 Pessac, France*
[d] *IMMO, UMR CNRS-Université d'Angers, 2, bd. Lavoisier, 49045 Angers, France*

Received 3rd December 1998, Accepted 10th February 1999

Electrocrystallization of three hydroxylated donor molecules derived from tetrathiafulvalene (TTF) or ethylenedithiotetrathiafulvalene (EDT-TTF), *i.e.* $Me_3TTF\text{-}CH_2OH$, $EDT\text{-}TTF(CH_2OH)_2$ and $TTF(CH_2OH)_4$, in the presence of $[n\text{-}Bu_4N^+]_2[Mo_6O_{19}]^{2-}$ afforded 2:1 cation radical salts, $[donor^{+\bullet}]_2[Mo_6O_{19}]^{2-}$, whose crystal structures have been solved by X-ray diffraction. In the three different salts complex hydrogen bond networks develop in the solid state where the oxygen atoms of both the hydroxyl groups and the $[Mo_6O_{19}]^{2-}$ anions act as hydrogen bond acceptors. The observed hydrogen bonding directed toward one surface, bridging oxygen atom of $[Mo_6O_{19}]^{2-}$ is rationalized by an analysis of *ab initio* calculations of the distribution of electrostatic potentials.

Introduction

Electroactive molecular materials based on polyoxometalates with a variety of sizes, shapes and spin states have been actively investigated in the past ten years and this topic has been recently reviewed.[1] For example, following our report[2] on $[BEDT\text{-}TTF]_8[SiW_{12}O_{40}]$, Coronado and co-workers[3] described a series of salts, isostructural to the former, and where the delocalized electrons of the conducting mixed-valence BEDT-TTF slabs coexist with the localized magnetic moments of the paramagnetic anions $[XW_{12}O_{40}]^{n-}$, $X = Cu^{II}$ ($n = 6$), Co^{II} ($n = 6$) or Fe^{III} ($n = 5$).[3] In the latter the magnetic atom hidden within the core of the heteropolyanion does not interact with the conducting π slabs. In the series[4] $[BEDT\text{-}TTF]_8[X^{n+}Z^{m+}\text{-}(H_2O)M_{11}O_{39}]^{(12-n-m)-}$ ($X = P^V$ or Si^{IV}; $M = Mo^{VI}$ or W^{VI}; $Z = Fe^{III}$, Cr^{III}, Mn^{II}, . . ., *etc.*), where the magnetic center is introduced on the outer shell of the polyanion, polymerized polyanion networks or positional disorder of the paramagnetic Z center are observed with no evidence for any sizeable magnetic interaction between the cationic slabs and the anions. This appears to be a general feature of all such organic–inorganic constructions associating "classical" organic π-donor molecules, *i.e.* TTF, TMTTF, TMTSF, BEDT-TTF, BEDS-TTF or BET-TTF† and polyoxoanions such as $[Mo_6O_{19}]^{2-}$.[5,6]

Several tetrathiafulvalene-based molecules bearing competing hydrogen bond donor and/or acceptor capabilities were recently described and engaged in cation radical salts. Examples include alcohols[7,8] in $Me_3TTF(CHMeOH)$ and $EDT\text{-}TTF(CH_2OH)$, phosphonate anions[9] in $Me_3TTF\text{-}PO_3H^-$ and the zwitterionic $[Me_3TTF\text{-}PO_3H^-]^{+\bullet}$ and thioamides[10] in TTF-CSNHMe. The architectures of the salts based on these multifunctional redox precursors result from a delicate yet effective balance between the requirements of the mode of overlap of the open-shell conjugated π systems and those of the (transverse) hydrogen bonds directed towards the inorganic anions. Such principles are further illustrated and rationalized in this paper where novel constructions based on the hydroxymethyl-functionalized TTF and EDT-TTF cores and the Linquist anion $[Mo_6O_{19}]^{2-}$ are discussed.

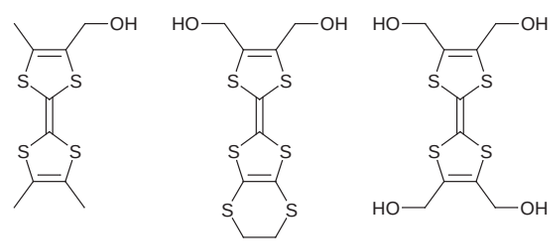

$Me_3TTF(CH_2OH)$ $EDT\text{-}TTF(CH_2OH)_2$ $TTF(CH_2OH)_4$

Electrocrystallization[11] of the mono-, di- and tetrahydroxylated donor molecules $Me_3TTF(CH_2OH)$, $EDT\text{-}TTF(CH_2OH)_2$ and $TTF(CH_2OH)_4$ in the presence of $[n\text{-}Bu_4N^+]_2[Mo_6O_{19}]^{2-}$ led to 2:1 salts, $[donor]_2[Mo_6O_{19}]$, whose crystal structures, hydrogen bonding pattern and magnetic properties are described and analysed in this paper. The capacity of $[Mo_6O_{19}]^{2-}$ to act as a hydrogen bond acceptor will be demonstrated by electrostatic potential distribution (ESP) calculations, conducted on $[Mo_6O_{19}]^{2-}$ and its hypothetical protonated form, $[HMo_6O_{19}]^-$.

† TTF = Tetrathiafulvalene; TMTTF = tetramethyltetrathiafulvalene; TMTSF = tetramethyltetraselenafulvalene; BEDT-TTF = bis(ethylenedithio)tetrathiafulvalene; BEDS-TTF = bis(ethylenedithio)tetraselenafulvalene and BET-TTF = bis(ethylenethio)tetrathiafulvalene.

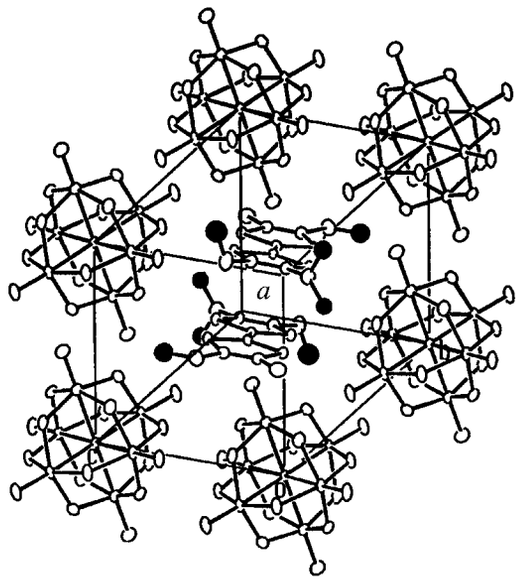

Fig. 1 A view of the unit cell of $[Me_3TTF(CH_2OH)]_2[Mo_6O_{19}]$. The four positions occupied by the disordered O atom have been darkened.

Results

The parent hydroxymethyl substituted tetrathiafulvalene, TTF-CH_2OH, was first described by Green[12] as an unstable compound prepared by reduction of the corresponding aldehyde, TTF-CHO. We reported that methyl substituted tetrathiafulvalenes such as Me_3TTF afforded more stable derivatives and could easily be lithiated as TTF itself for further derivatization.[7] Accordingly, Me_3TTF was lithiated with lithium diisopropyl amide and treated with *N*-methylformanilide to afford the corresponding aldehyde in good yield. Reduction with $NaBH_4$ in EtOH gives $Me_3TTF(CH_2OH)$.[13] The 3,4-(ethylenedithio)-3,4-bis(hydroxymethyl)tetrathiafulvalene EDT-TTF-$(CH_2OH)_2$ and the tetrakis(hydroxymethyl)tetrathiafulvalene $TTF(CH_2OH)_4$ were analogously obtained by reduction of the corresponding di- and tetra-aldehyde, as previously described.[14,15] Owing to the limited solubility of those hydroxylmethylated donor molecules in common organic solvents, electrocrystallizations had to be conducted in specific solvents or solvent mixtures (PhCN, MeCN–EtOH or DMF) at higher temperatures (see Experimental section).

$[Me_3TTF\text{-}CH_2OH]_2[Mo_6O_{19}]$

As shown in Fig. 1, the $[Mo_6O_{19}]^{2-}$ anions are located on inversion centers at the edges of the triclinic unit cell while an inversion centered organic dimer sits at the center of the unit cell, a structural organization which can be described as CsCl type, observed in cation radical salts of organic donors with similar large all-inorganic anions such as $[Re_6S_5Cl_9]^-$ or $[Mo_6Cl_8(NCS)_6]^{2-}$, in $[TMTSF]_2[Re_6S_6Cl_8]$[16] or $[TTF(SMe)_4]_2$-$[Mo_6Cl_8(NCS)_6]$.[17] One should note that the bridging oxygen atoms in $[Mo_6O_{19}]^{2-}$ are not equidistant from the flanking Mo atoms and O–Mo bond distances cluster into two groups, around 1.85–1.90 and 1.96–1.99 Å, respectively. This distortion, reported in the first structural determination of the $[Mo_6O_{19}]^{2-}$ anion,[18] is observed here and in the following two structures. Within the organic dimer, each molecule is oxidized to the cation radical and adopts a characteristic boat conformation with a limited folding of the dithiole rings along the S···S axis, by 5.1(1)° along S1···S2 and 2.0(1)° along S3···S4, a short plane-to-plane intermolecular distance, 3.272(4) Å, and a nearly eclipsed conformation. The oxygen atom of the hydroxyl group is found to be disordered on four different positions associated with three carbon atoms (C7, C8, C9). As a consequence, the hydroxyl hydrogen atom could not be located on

Table 1 Shortest intermolecular $O_{donor}\cdots O_{anion}$ distances (Å) in $[Me_3TTF(CH_2OH)]_2[Mo_6O_{19}]$

O7A···O13^{I}	2.78(2)	O7B···O3^{II}	2.92(2)
O7B···O1^{III}	3.05(2)	O8···O3^{II}	2.85(1)
O9···O32	2.90(1)		

I $1 + x, y, z$; II $x, y, -1 + z$; III $1 - x, 2 - y, 1 - z$.

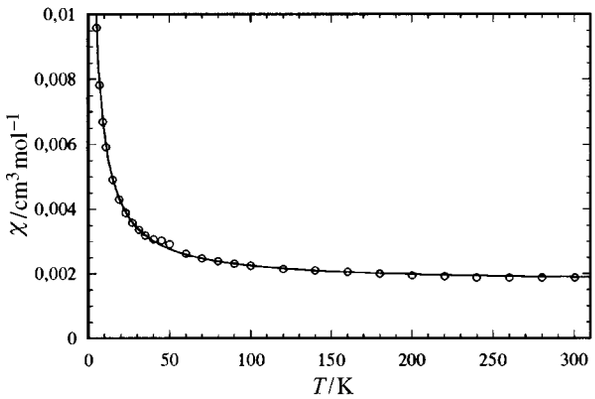

Fig. 2 Temperature dependence of the magnetic susceptibility of $[Me_3TTF(CH_2OH)]_2[Mo_6O_{19}]$.

Fourier difference maps and the analysis of hydrogen bonding in this salt will only rely on short intermolecular O···O distances. Indeed, as shown in Table 1, each of the four partially occupied hydroxyl sites is found to be engaged in a short $O_{donor}\cdots O_{anion}$ contact, between 2.78 and 3.05 Å, with the terminal and bridging oxygen atoms of the $[Mo_6O_{19}]^{2-}$ polyanion only, namely O3 and O13, O32, respectively while no short $O_{donor}\cdots O_{donor}$ short contacts could be identified. Those donor–anion close contacts can be compared for example with a similar hydrogen bond interaction identified between the hydroxyl group of EDT-TTF(CH_2OH) and the perrhenate anion ReO_4^- where a single O···O contact was observed at the longer 3.33 Å distance.[8] The $[Me_3TTF\text{-}CH_2OH^{+\bullet}]_2$ dimers are not fully isolated from each other but form weakly interacting stacks along the [100] direction. Indeed, calculated interaction energies[19] (from extended Hückel calculations with double-ζ orbitals for C, S and O) between two neighboring Me_3TTF-$CH_2OH^{+\bullet}$ cation radicals amount to 0.89 eV for the interaction within the dimer and 0.21 eV for the interaction between dimers. Therefore, the two radical species are associated in the strongly stabilized bonding combination of the HOMO of each $Me_3TTF\text{-}CH_2OH$ molecule and one expects the salt to be diamagnetic. A unique resonance line centered at $g = 2.0006$ is however observed by EPR spectroscopy on a single crystal, a value characteristic of TTF-based organic radicals, and attributed to magnetic defects. Its linewidth (ΔH) decreases from 7 G at room temperature to 4 G at 250 K and is constant down to 4 K, while the temperature dependence of the integrated spin susceptibility shows a Curie–Weiss behavior with a small deviation at higher temperatures, as confirmed by the SQUID susceptibility temperature dependence, well represented by the Curie–Weiss law, $\chi = \chi_0 + [C/(T - \theta)]$, with $C = 0.055$ cm^3 K mol^{-1} and $\theta = -2$ K (Fig. 2).

$[EDT\text{-}TTF(CH_2OH)_2]_2[Mo_6O_{19}]$

This salt crystallizes in the monoclinic system, space group $P2_1/c$, and the asymmetric unit consists of one $[Mo_6O_{19}]^{2-}$ polyanion, in general position, and two independent (A and B) EDT-TTF$(CH_2OH)_2$ molecules. Note that one of every two hydroxyl groups is found to be disordered on two positions. Thus, and despite the low-temperature X-ray data collection, hydrogen atoms could not be identified on the Fourier difference map. The two organic molecules organize into dimers

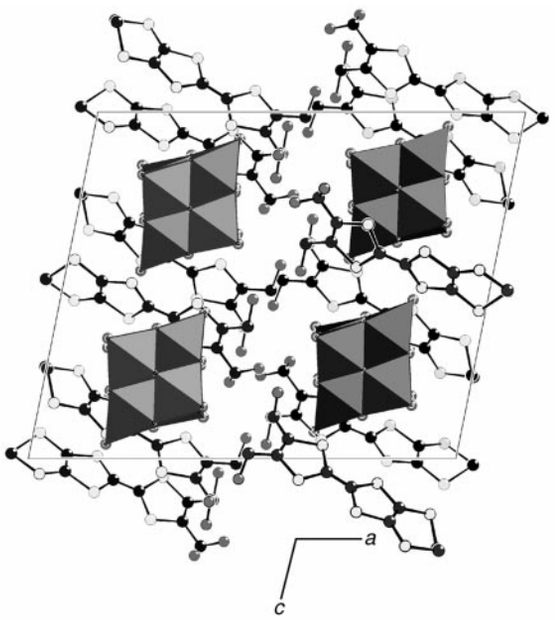

Fig. 3 Projection along the *b* axis of [EDT-TTF$(CH_2OH)_2]_2[Mo_6O_{19}$] showing the segregation of the disordered hydroxyl groups into layers.

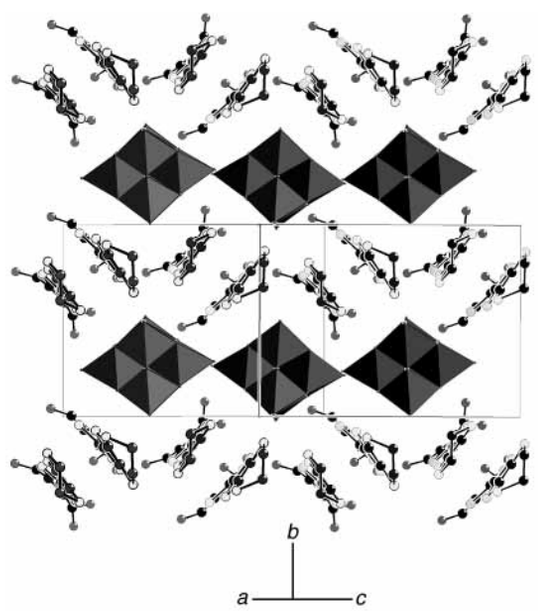

Fig. 4 A view of the mixed organic–inorganic plane in [EDT-TTF$(CH_2OH)_2]_2[Mo_6O_{19}$].

(Fig. 3), with a short plane-to-plane distance (3.31 Å) and a folding [along S1A···S2A 6.6(3), S3A···S4A 7.5(1), S1B···S2B 5.6(3) and S3B···S4B 5.2(1)°] of the dithiole rings away from each other (boat conformation). This structure, observed above in [Me_3TTF$(CH_2OH)]_2[Mo_6O_{19}$], is characteristic of fully oxidized, dicationic TTF dimers, as confirmed by the calculated interaction energy between the HOMOs of the two molecules, to 0.8 eV. No EPR signal was observed for this salt, a consequence of the strongly dimerized structure and the absence of any sizeable interdimer overlap interaction. In the solid state the segregation of the hydrophilic CH_2OH and hydrophobic SCH_2CH_2S outer ends of the organic donor molecules leads to a pattern of segregated slabs, a motif already encountered with phosphonate-substituted tetrathiafulvalenes.[9] A complex hydrogen bond network develops within the hydrophilic layer and involves the hydroxyl groups of the donor molecules as well as oxygen atoms of the $[Mo_6O_{19}]^{2-}$ anion. Short O···O contacts are indeed identified within dimers, with the neighboring ones and with oxygen atoms of the polyanion (Table 2). Note that the shortest $O_{donor}\cdots O_{anion}$ distances

Table 2 Shortest intermolecular O···O distances (Å) in [EDT-TTF$(CH_2OH)_2]_2[Mo_6O_{19}$]

Intradimer interactions			
O1A1···O1B1	2.60(2)	O1A2···O1B1	2.85(2)
Interdimer interactions			
O2A···O2B^{I}	2.66(1)	O2A···O2A^{I}	2.84(2)
O1B2···O2B^{II}	2.69(2)	O1A1···O2B^{III}	2.86(2)
Dimer–Mo_6O_{19} interactions			
O1B2···O35	2.70(2)	O1B1···O35	2.82(2)
O1A1···O3	2.89(2)	O1B2···O5	2.96(2)

I $1-x, -1-y, -z$; II $1-x, -y, -z$; III $x, -\frac{1}{2}-y, \frac{1}{2}+z$.

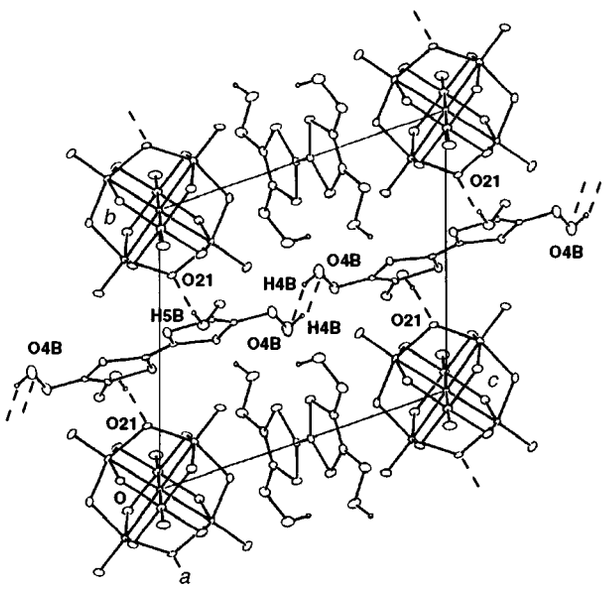

Fig. 5 A projection of the structure of [TTF$(CH_2OH)_4]_2[Mo_6O_{19}$] along the *a* axis. Both $[Mo_6O_{19}]^{2-}$ and TTF$(CH_2OH)_4^{+\bullet}$ moieties are located on inversion centers, at the corners of the cell and the center of the edges respectively. Note the hydrogen bond H4B···O4B cyclic motif as well as the H5B···O21 donor–polyanion hydrogen bond.

involve the bridging O35 atom, in contrast with the longer distances observed with the terminal O3 and O5 atoms. Within a layer (Fig. 4), $[Mo_6O_{19}]^{2-}$ dianions and orthogonal dicationic organic dimers alternate and the whole structure can be described as belonging to the NaCl structural type.

[TTF$(CH_2OH)_4]_2[Mo_6O_{19}$]

Considering that the single hydroxyl group appears disordered on three different methyl carbon atoms in [Me_3TTF-$(CH_2OH)]_2[Mo_6O_{19}$], it was anticipated that an ordered, eventually isostructural salt could be obtained by engaging the tetrakis(hydroxymethyl)tetrathiafulvalene TTF$(CH_2OH)_4$ with the same counter anion. Although electrocrystallization experiments with this tetrahydroxylated donor molecule proved difficult because of its very limited solubility in common solvents, a few crystals were obtained in DMF. The salt crystallizes in the triclinic system, space group $P\bar{1}$. One $[Mo_6O_{19}]^{2-}$ anion and two crystallographically independent radical cations are located on inversion centers (Fig. 5). The hydroxyl groups are now fully ordered and hydrogen atoms were unambiguously identified in Fourier difference maps, allowing for a precise analysis of the hydrogen bonding pattern. Indeed, as shown in Table 3, each of the four independent H atoms of the hydroxyl groups is engaged in one and only one hydrogen bond. Note also that the O···O distances are comparable to those revealed in the two former structures, confirming the hydrogen bond character of O···O interactions identified above in [Me_3-

Table 3 Hydrogen bond geometrical characteristics in $[TTF(CH_2OH)_4]_2[Mo_6O_{19}]$

	O···O/Å	H···O/Å	O–H···O/°
O5A–H5A···O5B^{I}	2.738(5)	1.934	166.4
O4A–H4A···O5A^{II}	2.778(5)	1.977	165.3
O5B–H5B···O21^{III}	2.873(6)	2.058	173.1
O4B–H4B···O4B^{IV}	2.895(5)	2.137	153.7

I $1 + x, y, z$; II $1 - x, -y, 1 - z$; III $-1 - x, 1 - y, 1 - z$; IV $-x, 1 - y, 1 - z$.

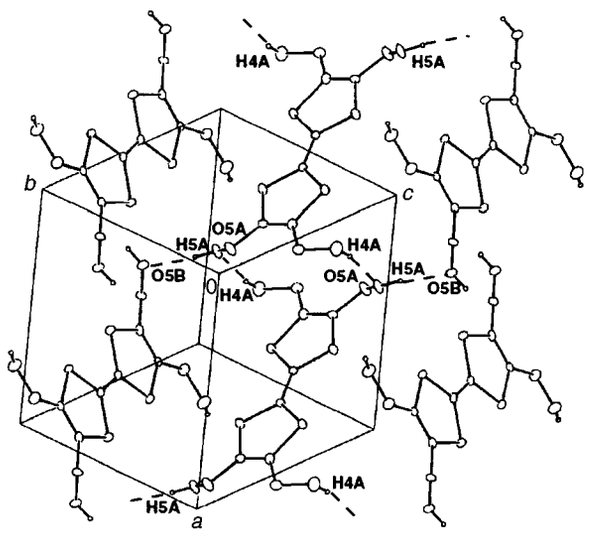

Fig. 6 A view along the $b + c$ direction of the donor plane showing the H4A···O5A and H5A···O5B hydrogen bond network.

$TTF(CH_2OH)]_2[Mo_6O_{19}]$ and $[EDT\text{-}TTF(CH_2OH)_2]_2[Mo_6O_{19}]$. Three hydrogen atoms are engaged in a bond with oxygen atoms of the CH_2OH groups while one and only one out of the four becomes bonded to a bridging oxygen atom (O21) of the polyanion. As shown in Fig. 5, molecules B are engaged in an inversion centered O4B–H4B···O4B′ motif which develops along the *c* axis while hydrogen atom H5B is engaged in a hydrogen bond with the bridging O21 atom of the $[Mo_6O_{19}]^{2-}$ anion. Fig. 6 shows the organic slab which develops perpendicular to the $b + c$ direction where molecules A are connected to each other along the *a* axis through the O4A–H4A···O5A hydrogen bond while the H5A atom links those columns with B molecules. Of particular note is the co-operative effect associated with all those hydrogen bonds as observed here in two extended motifs, a cyclic one ···O4B–H4···O4B′–H4B′··· (Fig. 5) and a linear one O4A–H4A···O5A–H5A···O5B–H5B···$O21_{anion}$ (Fig. 6). This co-operativity, often encountered with hydroxyl groups and particularly in carbohydrates,[20] has been shown substantially to increase the stability of such arrays.

Discussion

It is striking that in both $[Me_3TTF(CH_2OH)]_2[Mo_6O_{19}]$ and $[EDT\text{-}TTF(CH_2OH)_2]_2[Mo_6O_{19}]$ the organic π donor radical cations are strongly dimerized with intermolecular S···S distances as short as 3.32(2) Å and the hydroxyl groups disordered onto several positions with no clear hydrogen bond pattern. By contrast, in $[TTF(CH_2OH)_4][Mo_6O_{19}]$ the tetrahydroxylated cation radicals are orthogonal to each other and do not overlap. Instead, a precise, ordered, O–H···O hydrogen bond network is identified and connects the alternating organic and inorganic ions. Thus, from two principal competing interactions, namely (i) the overlap interaction of open-shell cation radicals which stabilizes the formation of strongly associated, eclipsed donor dimers, and (ii) the directional O–H···O hydrogen bonds, the electronic stabilization, and dimer formation, clearly prevails over the hydrogen-bond interactions when solely one and two hydroxyl groups are present on the TTF core. A similar dimer formation was also observed in $[TMTTF]_2[Mo_6O_{19}]$,[6] where no hydroxyl groups are present. This behaviour can be tentatively rationalized by a simple estimation of the energies involved in those two competing interactions. Indeed the O–H···O hydrogen bond energy[21] is estimated between 15 and 20 kJ mol^{-1}, *i.e.* between 0.15 and 0.20 eV, to be compared with the overlap stabilization of the radical cation within a dimer, which amounts to 0.35 to 0.5 eV per molecule. It therefore appears that the stabilization energy provided by one or two hydrogen bonds cannot compete favorably with the dimer formation. Conversely, the set of four ordered hydrogen bonds per donor molecule identified in $[TTF(CH_2OH)_4]_2[Mo_6O_{19}]$ provides sufficient intermolecular interaction energy to prevent the formation of discrete dimers.

In two of the three structures described above the oxygen atoms of the hydroxyl groups were found to be disordered on several positions. Beside the subsequent practical difficulty in locating the hydrogen atoms in Fourier difference maps, the occurrence of significant disorder indicates that the oxygen atoms of the $[Mo_6O_{19}]^{2-}$ anion exhibit no particularly strong hydrogen bond acceptor character. This was deduced earlier by Barcza and Pope[22] from their investigation of the stability constants in solution of 1:1 adducts of several polyanions with the chloral hydrate $[Cl_3CCH(OH)_2]$, a strong hydrogen bond donor. In $[TTF(CH_2OH)_4]_2[Mo_6O_{19}]$ where no disorder is encountered and where hydrogen atoms were unambiguously identified, one of the four independent H atoms was however found to be engaged in a hydrogen bond with $[Mo_6O_{19}]^{2-}$ while the three others are hydrogen-bonded to oxygen atoms of the CH_2OH groups, as observed in the crystal structures of a variety of alcohols. In the competition between hydroxylic and $[Mo_6O_{19}]^{2-}$ oxygen atoms the former are clearly better hydrogen-bond *acceptors*. Nevertheless, polyoxoanions prove to be able also to engage in hydrogen bonds.[23]

The two different kinds of oxygen atoms at the surface of the $[Mo_6O_{19}]^{2-}$ polyanion, namely the bridging and terminal ones, do not behave similarly since the shortest hydrogen bonds identified in the three structures involve almost exclusively bridging oxygen atoms. Indeed as reported by Barcza and Pope,[22] "the terminal oxygen atoms are strongly polarized toward the interior of the anion by π bonding to the metal atoms". Similar observations on the relative basicities of oxygen sites in polyanions were derived from *ab initio* studies[24] of a variety of polyoxometalates such as $[V_{10}O_{28}]^{6-}$ and its protonated derivative $[H_3V_{10}O_{28}]^{3-}$.[25] In order to rationalize the above experimental observations, the distribution of electrostatic potentials (ESP) was determined by *ab initio* calculations on the $[Mo_6O_{19}]^{2-}$ anion.[19] The electrostatic potential distribution has been displayed in two different sections of the anion, one containing four Mo, four bridging, four terminal as well as the central O atoms (Fig. 7, top) and one containing three bridging and three terminal O atoms (Fig. 7, bottom). It is clearly seen that the deepest minima in any of these planes are located in the neighborhood of the bridging O atoms, at an altitude of about 1.2 Å from those atoms in the first plane (Fig. 7, top). Therefore, one expects that the protonation of $[Mo_6O_{19}]^{2-}$ would specifically occur on those bridging O atoms.

If we now consider the possible localization of a hydrogen bond donor at the proximity of the anion surface, the situation is much less clear-cut. Considering that the observed (O)H···O_{anion} distances amount to ≈2 Å, the former deep potential minima are probably not so pertinent anymore. The electrostatic potential distribution has thus been calculated in a plane parallel to the triangular face of the $[Mo_6O_{19}]^{2-}$ anion, at respectively 1.1 (Fig. 8, top) and 2.2 Å (Fig. 8, bottom) away

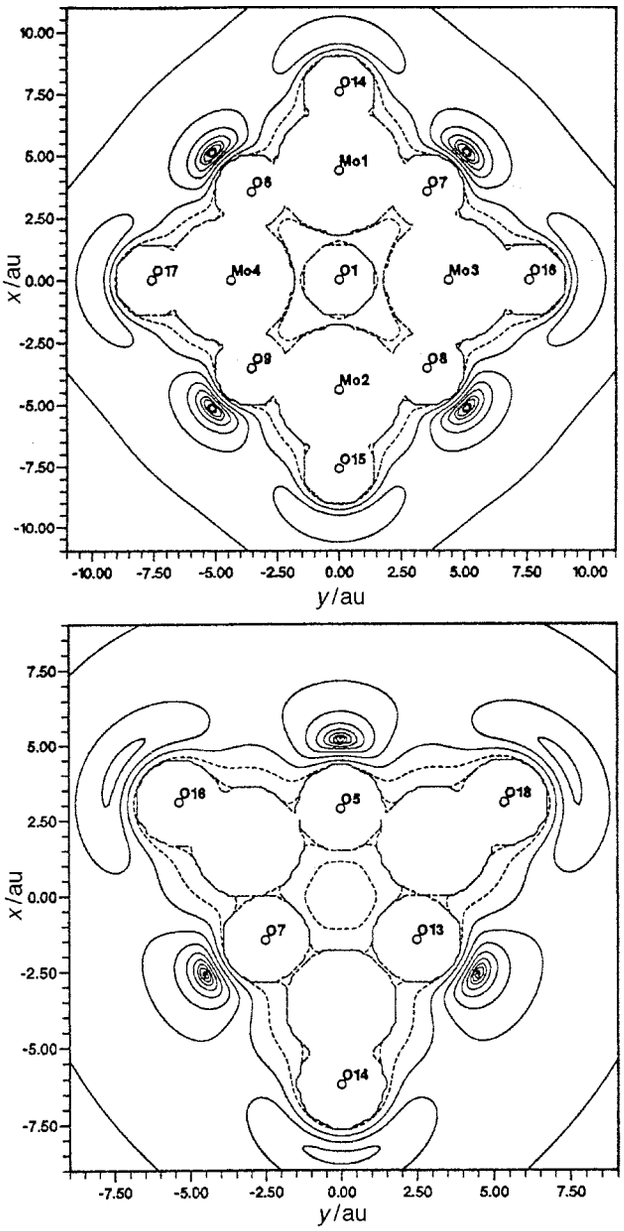

Fig. 7 Sections of the electrostatic potentials for $[Mo_6O_{19}]^{2-}$, in the plane containing four Mo, four terminal and four bridging O atoms (top) and in the plane containing three terminal and three bridging O atoms (bottom). Lowest contour: −0.27835 hartree (top), −0.26646 hartree (bottom). First contour interval: 5×10^{-5} hartree (top), 4×10^{-5} hartree (bottom). Successive contour intervals increased by a factor of 2 in both sections.

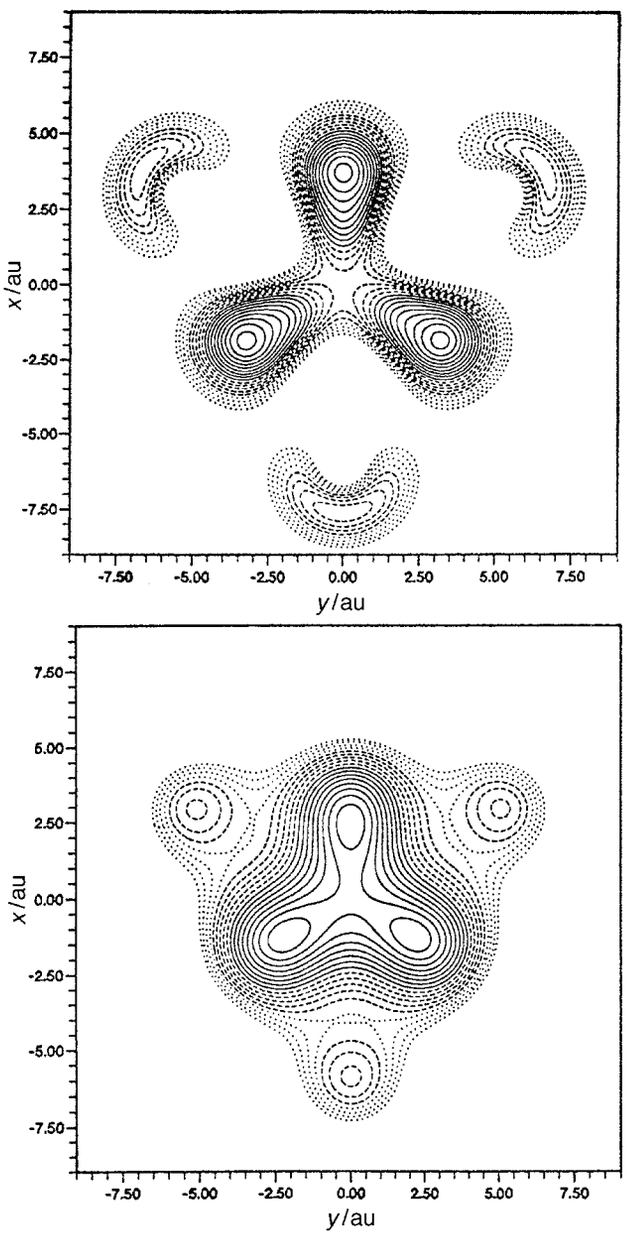

Fig. 8 Sections of the electrostatic potentials for $[Mo_6O_{19}]^{2-}$, away from the triangular anion face containing three terminal and three bridging O atoms at $z = 1.1$ Å (top) and 2.2 Å (bottom) respectively. Lowest contour: −0.285 hartree (top), −0.220 hartree (bottom). All contour intervals equal to 0.003 hartree (top), 0.001 hartree (bottom).

from the surface. While the three deep minima are indeed found at a short distance (1.1 Å) from the surface on the three bridging oxygen atoms, they merge into a deep shallow zone delocalized between the three bridging O atoms at larger distances (2.2 Å) from the surface. As a consequence, we expect weakly acidic hydrogen atoms approaching a face of the anion to be mainly attracted by an extended array rather than by a specific O bridging atom.

It is also of interest to evaluate the effect of an approaching H atom on the electrostatic potential distribution of the anion. Similar calculations were conducted on the hypothetical $[HMo_6O_{19}]^-$ anion with the H atom co-ordinated to a bridging O atom at a 1.1 Å distance and located in a plane containing four Mo atoms. As shown in Fig. 9, protonation of O7 strongly modifies the electrostatic potentials of the neighboring O atoms. It particularly decreases the minima of the bridging O6 and O8 atoms (Fig. 9, top) while the O5 and O13 atoms pertaining to the same triangular face are much less affected (Fig. 9, bottom). Note also that a secondary minimum now appears on the *terminal* O18 atom also pertaining to the same triangular face (Fig. 9, bottom). This effect is more clearly seen while going away from the triangular face of the anion as described above for $[Mo_6O_{19}]^{2-}$. Indeed, as shown in Fig. 10 when moving away from the same triangular face described in Fig. 9 (bottom), the minima associated with the bridging O5, O13 atoms and with the terminal O18 atom are both clearly identified at 1.1 Å from the surface (Fig. 10, top) while at 2.2 Å the strongest minimum is associated with the terminal O18 atom (Fig. 10, bottom).

We can therefore conclude from those calculations that (i) the bridging O atoms are definitely the most basic ones in $[Mo_6O_{19}]^{2-}$, (ii) hydrogen bond donors experience at 2–2.2 Å from the oxide surface a shallow negatively charged zone located at the center of the triangular faces of the anion and (iii) protonation of the anion strongly modifies the potential

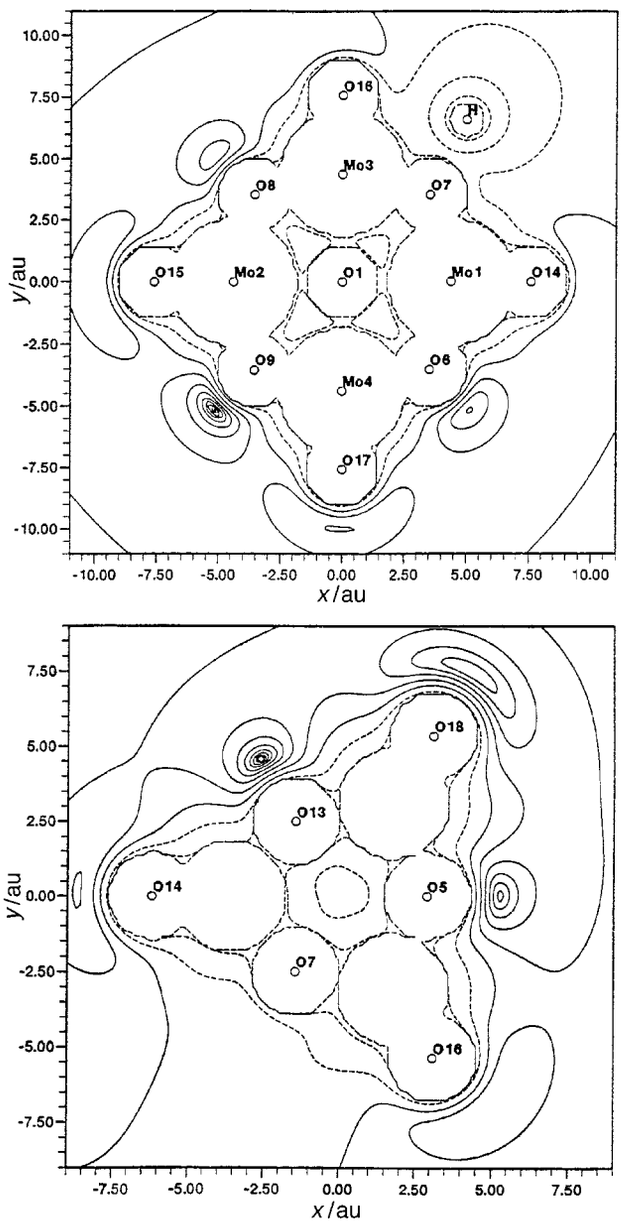

Fig. 9 Sections of the electrostatic potentials for the hypothetical $[HMo_6O_{19}]^-$, in the plane containing four Mo, four terminal and four bridging O atoms (top) and in the plane containing three terminal and three bridging O atoms (bottom); the H atom is linked to O7 which pertains to both planes. Lowest contour: −0.18092 hartree (top), −0.15167 hartree (bottom). First contour interval: 4×10^{-5} hartree. Successive contour intervals increased by a factor of 2.

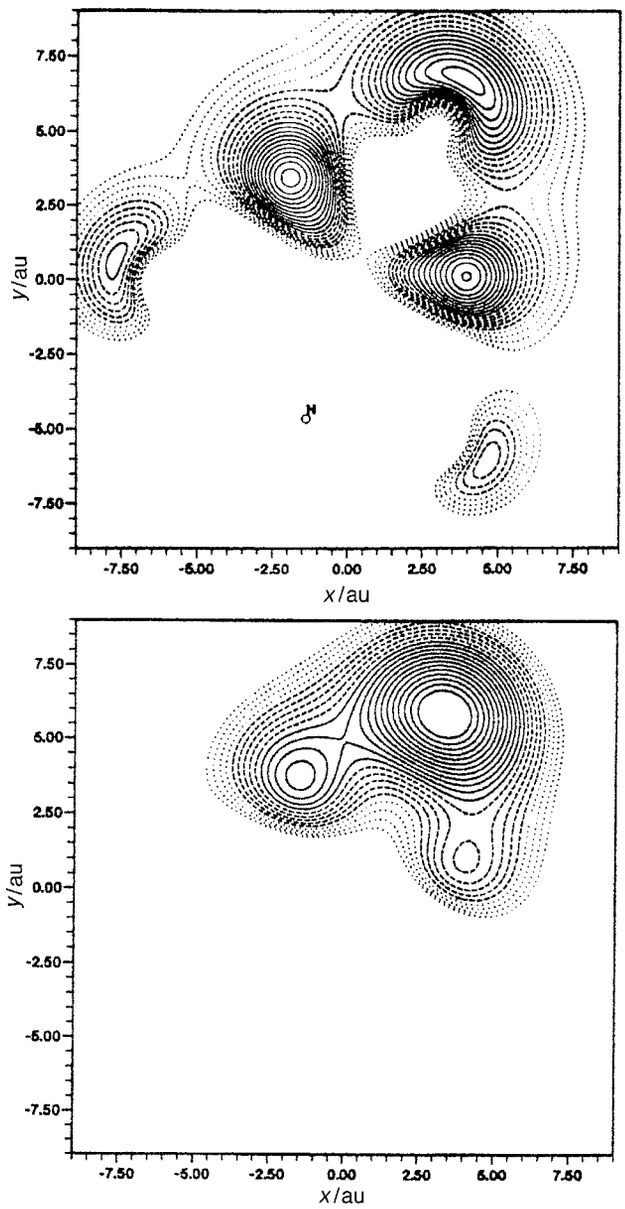

Fig. 10 Sections of the electrostatic potentials for the hypothetical $[HMo_6O_{19}]^-$, away from the triangular anion face containing three terminal and three bridging O atoms at $z = 1.1$ Å (top) and 2.2 Å (bottom) respectively. Lowest contour: −0.160 hartree (top), −0.11-hartree (bottom). All contour intervals equal to 0.003 hartree (top)-0.001 hartree (bottom)

distribution and eventually makes terminal O atoms available for further interaction with electrophilic moieties.

In their interaction with hydrogen bond donors such as hydroxyl groups, surface O atoms of $[Mo_6O_{19}]^{2-}$ are in competition with the O atoms of the hydroxyl groups which exhibit stronger hydrogen-bond acceptor capabilities. Further work along those lines could therefore involve H-donor molecules with no competing acceptor atoms such as for example tetrathiafulvalenes bearing ammonium groups. Indeed, crystalline alkylammonium (RNH_3^+, $R_2NH_2^+$) polyoxometalates have been shown to exhibit photochromism upon UV irradiation ($\lambda \leq 400$ nm), a process involving the transfer of a proton from a *hydrogen-bonded* alkylammonium nitrogen to a *bridging oxygen* atom at the photoreducible site in the edge-shared MoO_6 octahedral lattice.[26] Modifications of the $[Mo_6O_{19}]^{2-}$ anion itself could also be considered in order to increase the total charge and/or the charge density on the surface O atoms as in $[Mo_6O_{18}(NO)]^{3-}$ for example.[27]

Experimental

Synthesis of 3-formyl-4,3′,4′-trimethyltetrathiafulvalene

To a solution of Me_3TTF[7] (1 g, 4.06 mmol) in dry Et_2O (100 mL) at −78 °C under nitrogen was added $NH(i\text{-}Pr)_2$ (0.64 mL, 4.46 mmol) followed by BuLi (2.5 M in hexanes, 1.8 mL, 4.46 mmol). The yellow suspension was stirred for 1 h and *N*-methylformanilide (0.54 mL, 4.46 mmol) added. The reaction mixture was slowly warmed to room temperature and hydrolysed with acidified water (0.01 M HCl, 50 mL) giving rise to a dark red solution. This was extracted with toluene, washed with 0.01 M HCl, water and dried with $MgSO_4$. Chromatography on SiO_2 (toluene) afforded the required compound as a red product, recrystallized from acetone, yield 0.7 g (63%) mp 170–171 °C [Calc. for $C_{10}H_{10}OS_4$ (Found): C, 43.75 (44.47); H, 3.68 (3.82); O, 5.83 (5.81); S, 46.72 (45.93)%]. ^{1}H NMR ($CDCl_3$, TMS): δ 1.93 (s, 6 H, Me), 2.15 (s, 3 H, Me) and 9.70 (s, 1 H, CHO). UV(DMF): $\lambda_{max} = 446$ nm.

Table 4 Crystallographic data for the three 2:1 salts with $[Mo_6O_{19}]^{2-}$

Donor molecule	$Me_3TTF\text{-}CH_2OH$	$EDT\text{-}TTF(CH_2OH)_2$	$TTF(CH_2OH)_4$
Formula	$C_{20}H_{24}Mo_6O_{21}S_8$	$C_{20}H_{20}Mo_6O_{23}S_{12}$	$C_{20}H_{24}Mo_6O_{27}S_8$
Formula weight	1432.51	1588.72	1528.51
Crystal dimensions/mm	0.4 × 0.2 × 0.1	0.21 × 0.11 × 0.02	0.28 × 0.05 × 0.02
Crystal system	Triclinic	Monoclinic	Triclinic
Space group	$P\bar{1}$	$P2_1/c$	$P\bar{1}$
a/Å	7.830(1)	20.654(2)	8.668(2)
b/Å	11.288(2)	11.5411(8)	10.862(2)
c/Å	11.375(2)	17.110(1)	11.478(2)
α/°	109.08(2)		69.58(3)
β/°	95.29(2)	101.342(9)	83.28(3)
γ/°	103.41(2)		77.00(3)
V/Å^3	908.8(3)	3998.8(5)	985.9(3)
Z	1	4	1
D_c/g cm^{-3}	2.617	2.639	2.574
μ/mm^{-1}	2.551	2.538	2.371
Data collected	9813	34134	10552
θ Range/°	2.0, 27	2.0, 26.9	2.04, 26.95
Independent reflections	3642	8212	3914
Obs. reflections [$I > 2\sigma(I)$]	3204	6918	2948
Parameters refined	257	543	277
Absorption correction	Empirical	Numerical	Numerical
T_{max}, T_{min}	0.793, 0.580	0.915, 0.640	0.991, 0.827
$R(F)$ [$I > 2\sigma(I)$]	0.0260	0.0637	0.0247
$wR(F^2)$ (all)	0.0797	0.1335	0.0403
Goodness of fit	1.051	1.292	0.89
Residual density/e Å^{-3}	1.28, −0.55	2.7, −1.5	0.57, −0.69

Synthesis of 3-(hydroxymethyl)-4,3′,4′-trimethyltetrathiafulvalene

The compound $Me_3TTF\text{-}CHO$ (0.7 g, 2.55 mmol) was suspended in EtOH (50 mL) and $NaBH_4$ (0.24 g, 6.37 mmol) added by fractions. The mixture was warmed to reflux for 30 min, cooled to room temperature and the solvent evaporated. Trituration of the solid residue with water and filtration afforded an orange solid, recrystallized from acetone, yield 0.66 g (94%), mp 203–204 °C [Calc. for $C_{10}H_{12}OS_4$ (Found): C, 43.44 (43.25); H, 4.38 (4.48); O, 5.79 (6.04); S, 46.38 (46.13)%]. ^{1}H NMR ($CDCl_3$, TMS): δ 1.93 (br s, 9 H, Me) and 4.23 (s, 2 H, CH_2). UV (DMF): λ_{max} = 476 nm.

Electrocrystallization conditions

The electrolyte, $[n\text{-}Bu_4N]_2[Mo_6O_{19}]$, was prepared as reported elsewhere[28] and recrystallized twice before use. The donor molecules were galvanostatically electrooxidized in 2 mM solutions of $[n\text{-}Bu_4N]_2[Mo_6O_{19}]$, in PhCN at 40 °C for $EDT\text{-}TTF(CH_2OH)_2$, in MeCN–EtOH (1:1) at 20 °C for $Me_3TTF\text{-}(CH_2OH)$ or in DMF at 30 °C for $TTF(CH_2OH)_4$. Crystals were harvested on the electrode after typically one week.

Crystallography

Crystallographic data for the three salts are summarized in Table 4. Data were collected on a Stoe Imaging Plate Diffraction System (IPDS) at 150 K with Mo-Kα radiation (λ = 0.71073 Å). Structures were solved by direct methods using SHELXS 86[29] and refined by full-matrix least-square procedures using SHELXL 93.[30] All non-hydrogen atoms were refined anisotropically except the disordered oxygen atoms found in $[Me_3TTF\text{-}CH_2OH]_2[Mo_6O_{19}]$ and in $[EDT\text{-}TTF(CH_2OH)_2]_2[Mo_6O_{19}]$. In the former the O atom is disordered on four positions with occupation parameters refined to values close to 1/3 on C8 and C9 and to 1/6 for the two partially occupied O sites linked to C7. These values were thus fixed and the isotropic thermal parameters of O8, O9 and O7A, O7B were then refined. In the $EDT(CH_2OH)_2$ salt one of every two O atoms of each independent donor molecules A and B was found disordered on two positions. Refinement of their occupation parameters converged to 0.6 and 0.4 for the two O positions linked to C1A, to 0.5 and 0.5 for the two O positions linked to C1B. These values were thus fixed and the isotropic thermal parameters of O1A1, O1A2, O1B1 and O1B2 refined. Furthermore, in this salt, atom C7A could not be refined anisotropically and was therefore refined with an isotropic thermal parameter. The strong residual peak in the Fourier difference map is located at 0.9 Å from atom Mo3. Hydrogen atoms of the methylene groups were introduced at calculated positions in $[EDT\text{-}TTF(CH_2OH)_2]_2[Mo_6O_{19}]$ and $[TTF(CH_2OH)_4]_2[Mo_6O_{19}]$, included in structure factor calculations and not refined (riding model); they were not introduced in $[Me_3TTF(CH_2OH)]_2[Mo_6O_{19}]$. Hydrogen atoms of the hydroxyl groups could not be found in Fourier difference maps for $[Me_3TTF(CH_2OH)]_2[Mo_6O_{19}]$ and $[EDT\text{-}TTF(CH_2OH)_2]_2[Mo_6O_{19}]$ but they were unambiguously identified in $[TTF(CH_2OH)_4]_2[Mo_6O_{19}]$ but not refined.

CCDC reference number 186/1353.

See http://www.rsc.org/suppdata/dt/1999/1241/ for crystallographic files in .cif format.

Magnetic measurements

The ESR spectra were recorded on a Varian X-band spectrometer operating at 9.3 GHz and equipped with an OXFORD ESR 900 helium cryostat. Magnetic susceptibility measurements for $[Me_3TTF(CH_2OH)]_2[Mo_6O_{19}]$ were performed on a Quantum Design MPMS-2 SQUID magnetometer operating in the range 1.7–300 K.

Acknowledgements

This work was supported by the Centre National de la Recherche Scientifique and the Région Pays de Loire.

References

1 E. Coronado and C. J. Gómez-García, *Chem. Rev.*, 1998, **98**, 273.
2 A. Davidson, K. Boubekeur, A. Pénicaud, P. Auban, C. Lenoir, P. Batail and G. Hervé, *J. Chem. Soc., Chem. Commun.*, 1989, 1373.
3 C. J. Gómez-García, L. Ouahab, C. Giménez-Saiz, S. Triki, E. Coronado and P. Delhaes, *Angew. Chem., Int. Ed. Engl.*, 1994, **33**, 223; C. J. Gómez-García, C. Giménez-Saiz, S. Triki,

E. Coronado, P. Le Maguéres, L. Ouahab, L. Ducasse, L. C. Sourisseau and P. Delhaes, *Inorg. Chem.*, 1995, **34**, 4139.
4 J. R. Galán-Mascarós, C. Giménez-Saiz, S. Triki, C. J. Gómez-García, E. Coronado and L. Ouahab, *Angew. Chem.*, *Int. Ed. Engl.*, 1995, **34**, 1460.
5 D. Attanasio, C. Bellitto, M. Bonamico, V. Fares and P. Imperatori, *Gazz. Chim. Ital.*, 1991, **121**, 155; S. Triki, L. Ouahab, J. Padiou and D. Grandjean *J. Chem. Soc.*, *Chem. Commun.*, 1989, 1068.
6 S. Triki, L. Ouahab, D. Grandjean and J.-M. Fabre, *Acta Crystallogr.*, *Sect. C*, 1991, **47**, 1371.
7 A. Dolbecq, M. Fourmigué, P. Batail and C. Coulon, *Chem. Mater.*, 1994, **6**, 1413.
8 P. Blanchard, K. Boubekeur, M. Sallé, G. Duguay, M. Jubault, A. Gorgues, J. D. Martin, E. Canadell, P. Auban-Senzier, D. Jérome and P. Batail, *Adv. Mater.*, 1992, **4**, 579.
9 A. Dolbecq, M. Fourmigué, F. C. Krebs, P. Batail, E. Canadell, R. Clérac and C. Coulon, *Chem. Eur. J.*, 1996, **2**, 1275.
10 A. J. Moore, M. R. Bryce, A. S. Batsanov, J. N. Heaton, C. W. Lehmann, J. A. K. Howard, N. Robertson, A. E. Underhill and I. F. Perepichka, *J. Mater. Chem.*, 1998, **8**, 1541.
11 P. Batail, K. Boubekeur, M. Fourmigué and J.-C. P. Gabriel, *Chem. Mater.*, 1998, **10**, 3005.
12 D. C. Green, *J. Org. Chem.*, 1979, **44**, 1477.
13 See also A. J. Moore, M. R. Bryce, A. S. Batsanov, J. C. Cole and J. A. K. Howard, *Synthesis*, 1995, 675.
14 P. Blanchard, M. Sallé, G. Duguay, M. Jubault and A. Gorgues, *Tetrahedron Lett.*, 1992, **33**, 2685.
15 M. Sallé, A. Gorgues, M. Jubault, K. Boubekeur and P. Batail, *Tetrahedron*, 1992, **48**, 3081.
16 K. Boubekeur, Ph.D. Thesis, University of Rennes, 1989.
17 A. Guirauden, I. Johannsen, P. Batail and C. Coulon, *Inorg. Chem.*, 1993, **32**, 2446.
18 H. R. Allcock, E. C. Bissell and E. T. Shawl, *Inorg. Chem.*, 1973, **12**, 2963.
19 R. Hoffmann, *J. Chem. Phys.*, 1963, **39**, 1397.
20 G. A. Jeffrey, M. E. Gress and S. Takagi, *J. Am. Chem. Soc.*, 1977, **99**, 609; G. A. Jeffrey and L. Lewis, *Carbohydr. Res.*, 1978, **60**, 179.
21 G. A. Jeffrey and W. Saenger, *Hydrogen Bonding in Biological Structures*, Springer, Berlin, Heidelberg, 1991.
22 L. Barcza and M. T. Pope, *J. Phys. Chem.*, 1975, **79**, 92.
23 See also C. Rimbaud, L. Ouahab, J. P. Sutter and O. Kahn, *Mol. Cryst. Liq. Cryst.*, 1997, **306**, 67.
24 M.-M. Rohmer, M. Bénard, J.-P. Blaudeau, J.-M. Maestre and J.-M. Poblet, *Coord. Chem. Rev.*, 1998, **178**–**180**, 1019.
25 J.-Y. Kempf, M.-M. Rohmer, J.-M. Poblet, C. Bo and M. Bénard, *J. Am. Chem. Soc.*, 1992, **114**, 1136.
26 T. Yamase, *Chem. Rev.*, 1998, **98**, 307.
27 A. Proust, R. Thouvenot, F. Robert and P. Gouzerh, *Inorg. Chem.*, 1993, **32**, 5299; A. Proust, R. Thouvenot, S.-G. Roh, J.-K. Yoo and P. Gouzerh, *Inorg. Chem.*, 1995, **34**, 4106.
28 M. Che, M. Fournier and J.-P. Launay, *J. Chem. Phys.*, 1979, **71**, 1954.
29 G. M. Sheldrick, *Acta Crystallogr.*, *Sect. A*, 1990, **46**, 467.
30 G. M. Sheldrick, SHELXL 93, Program for the Refinement of Crystal Structures, University of Göttingen, 1993.

Paper 8/09442J